

# On the $W+4$ jets background to the top quark asymmetry at the Tevatron

Kaoru Hagiwara<sup>a</sup>, Junichi Kanzaki<sup>b</sup>, Yoshitaro Takaesu<sup>a</sup>

<sup>a</sup>KEK Theory Center and Sokendai, Tsukuba, 305-0801, Japan

<sup>b</sup>KEK, Tsukuba, 305-0801, Japan

## Abstract

We investigate the possibility that the  $W+4$  jets background is a source of the anomalously large top-antitop ( $t\bar{t}$ ) charge asymmetry observed at the Tevatron. We simulate the  $t\bar{t}$  reconstruction of the signal and background events at the matrix-element level and find that the reconstructed  $t\bar{t}$  candidates from the  $W+4$  jets background could give large forward-backward asymmetry. We suggest serious re-evaluation of the  $W+4$  jets background for the  $t\bar{t}$  candidate events by studying the distributions of the reconstructed  $t\bar{t}$  systems in their rapidity difference, the transverse momentum of the top quark, and that of the  $t\bar{t}$  system, which can differ significantly from those of the QCD  $t\bar{t}$  production events especially at high  $t\bar{t}$  invariant mass.

## 1. Introduction

Since CDF[1] and D0[2] experiments reported the significant deviation from the next-to-leading order (NLO) prediction[3, 4, 5, 6] in the forward-backward asymmetry of top-antitop ( $t\bar{t}$ ) productions in  $p\bar{p}$  collisions, the origin of the discrepancy has been one of the serious issues in high-energy physics. Contributions from the NNLL QCD[7] and the QED higher order corrections[8] have been discussed, but they are not sufficient to explain the anomaly. Although both experiments seem to be confident that the large asymmetry is originated in the  $t\bar{t}$  signal events, there may be room for the background events to be responsible for the large positive asymmetry in view of the complexity of the experimental analysis and our imperfect understanding of multi-jet events at hadron colliders.

In this short report we investigate the possibility that the  $W+4$  jets background, the main background for the  $t\bar{t}$  production process, is a source of the disagreement in the top forward-backward asymmetry. We simulate the experimental event-selection cuts for the  $t\bar{t}$ -candidate events using the event samples generated with exact leading-order matrix elements. It is then found that the reconstructed  $t\bar{t}$  candidates from  $W+4$  jets background can give rise to the large forward-backward asymmetry, especially at high  $t\bar{t}$  invariant mass. We present kinematic distributions at the parton level because the smearing due to subsequent parton showering is not fully understood for multi-jet processes at hadron colliders, as hinted by the discrepancy in the di-jet invariant mass distribution in  $W+2$  jets

events studied at the Tevatron[9, 10]. The following results should hence be regarded as hints of what could be observed in real experiments after smearing due to QCD shower development and hadronization, detector resolutions, and event reconstruction complexities.

## 2. Event selection and reconstruction

In this section we summarize the parton-level event generation and the  $t\bar{t}$ -reconstruction procedures to obtain the  $t\bar{t}$  signal and its  $W+4$  jets background distributions. We use MadGraph[11] and its GPU version[12, 13, 14] to generate the following three sets of events:

$$p\bar{p} \rightarrow t\bar{t} \rightarrow (l^+ v_l b) (\bar{b} 2j), \quad (1)$$

$$p\bar{p} \rightarrow W^+ b\bar{b} 2j \rightarrow (l^+ v_l) b\bar{b} 2j, \quad (2)$$

$$p\bar{p} \rightarrow W^+ 4j \rightarrow (l^+ v_l) 4j, \quad (3)$$

where  $l$  is an electron or muon, while  $j$  can be a gluon or a light ( $u, d, s, c$ ) quark or antiquark. Sample (1) gives  $t\bar{t}$  signal events while (2) and (3) contribute to the  $W+4$  jets background. We use CTEQ6L1 parton distribution functions and set the renormalization and factorization scales at half of the  $t\bar{t}$  invariant mass ( $M_{t\bar{t}}$ ) for  $t\bar{t}$  events (1) and at 20 GeV for the  $W+4$  jets events (2) and (3). Although these are parton level samples, we regard each generated gluons and quarks as a jet. The generated  $t\bar{t}$  sample does not have NLO contributions and gives no forward-backward asymmetry. However, the asymmetry predicted by the Standard Model (SM) at NLO is less than the experimental resolutions of CDF and D0 experiments[1, 2], and hence we ignore QCD higher order corrections in this study.

Email addresses: kaoru.hagiwara@kek.jp (Kaoru Hagiwara), junichi.Kanzaki@cern.ch (Junichi Kanzaki), takaesu@post.kek.jp (Yoshitaro Takaesu)

Generated samples are then passed to the event selection procedure. Firstly they are required to satisfy the following kinematic cuts, which simulate the typical  $t\bar{t}$  event-selection cuts at the Tevatron[2]:

$$p_{Tj} > 20 \text{ GeV}, \quad |\eta_j| < 2.5, \quad (4a)$$

$$\max\{p_{Tj}\} > 40 \text{ GeV}, \quad (4b)$$

$$p_{Tl} > 20 \text{ GeV}, \quad |\eta_l| < 2.0, \quad (4c)$$

$$\Delta R_{jj} > 0.5, \quad \Delta R_{jl} > 0.5, \quad \Delta R_{ll} > 0.5, \quad (4d)$$

$$\not{p}_T > 20 \text{ GeV}, \quad (4e)$$

where  $p_T$  and  $\eta$  are the transverse momentum and pseudo-rapidity, respectively;  $j$  can be a gluon, quark or antiquark; and  $l$  represents an electron or muon. Here  $\Delta R_{ab}$  is the distance in the (pseudo-rapidity)-(azimuthal-angle) plane,

$$\Delta R_{ab} = \sqrt{(\eta_a - \eta_b)^2 + (\phi_a - \phi_b)^2}, \quad (5)$$

and  $\not{p}_T$  is defined as the magnitude of the three-momentum of the neutrino,

$$\not{p}_T = |\vec{p}_{Tv_l}|. \quad (6)$$

We then select  $t\bar{t}$  candidate events with a lepton + 4 jets + large  $\not{p}_T$  by requiring the following three conditions

$$\text{one electron or muon,} \quad (7a)$$

$$\text{at least 4 jets,} \quad (7b)$$

$$\text{one or two } b\text{-tagged jets.} \quad (7c)$$

When applying the requirement (7c), we assume 70%  $b$ -tagging efficiency and 8% probability of miss-identifying a light jet as a  $b$ -jet[2]. Therefore, 84.6% of the signal (1) and  $l\nu b\bar{b}2j$  background events (2) survive the condition (7c), while 31.4% of the  $l\nu 4j$  background events (3) remain. It turns out that the  $l\nu 4j$  events with one or two miss-tags give the dominant background to the  $t\bar{t}$  signal events.

We then reconstruct  $t\bar{t}$  pairs by following the constrained kinematic fit[2] employed in analyses of top physics at the Tevatron. The lepton, missing transverse momentum ( $\not{p}_T$ ) and leading four jets are used for the reconstruction. The neutrino  $\vec{p}_T$  is reconstructed as the missing  $\vec{p}_T$ , but its rapidity is not fully determined from the  $W$  mass constraint, leaving two possible neutrino four-momenta in the zero  $W$ -width limit. Two of the leading four jets are assigned to the  $b$  and  $\bar{b}$  quark while the others should form the  $W$  boson. In general, there are 24 possible combinations of the two neutrino momenta and jet assignments. By assigning a  $b$ -tagged jet to the  $b$  or  $\bar{b}$  quark, this number is reduced to twelve for single- $b$ -tag events, and to four for double- $b$ -tag events. Among all these possible combinations, we select one combination for the reconstructed  $t\bar{t}$  candidate by minimizing the  $\chi^2$  function[15] defined as

$$\begin{aligned} \chi^2 = & \left( \frac{M_{jj} - M_W}{\Gamma_W} \right)^2 + \left( \frac{M_{l\nu} - M_W}{\Gamma_W} \right)^2 + \left( \frac{M_{bjj} - M_t}{\Gamma_t} \right)^2 \\ & + \left( \frac{M_{bl\nu} - M_t}{\Gamma_t} \right)^2, \end{aligned} \quad (8)$$

where  $M_W, M_t, \Gamma_W, \Gamma_t$  are the mass and width of a  $W$  boson and top quark: 80.4 GeV, 172.5 GeV, 2.08 GeV and 1.35 GeV, respectively.  $M_{jj}, M_{l\nu}, M_{bjj}$  and  $M_{bl\nu}$  are the invariant mass of the two jets that are assigned to a  $W$  boson ( $W$  jets), the lepton-neutrino, the  $b$ - $W$  jets, and the  $b$ -lepton-neutrino system, respectively. The top and antitop quarks are identified by the lepton charge.

For each selected event, the rapidity difference ( $\Delta y$ ) between the reconstructed top and antitop quarks is defined as

$$\Delta y = y_t - y_{\bar{t}} = q(y_{t,\text{lep}} - y_{t,\text{had}}), \quad (9)$$

where  $q$  is the sign of the lepton charge, and  $y_{t,\text{lep}}$  and  $y_{t,\text{had}}$  are the rapidities of the leptonically and hadronically decayed top quarks, respectively. The forward-backward asymmetry is then defined as

$$A_{FB}^{t\bar{t}} = \frac{N(\Delta y > 0) - N(\Delta y < 0)}{N(\Delta y > 0) + N(\Delta y < 0)}, \quad (10)$$

where  $N(\Delta y > 0)$  and  $N(\Delta y < 0)$  are the number of events with positive and negative rapidity difference, respectively. This asymmetry is evaluated for the event samples (1), (2) and (3) separately.

### 3. Results

In this section we discuss kinematic distributions of the reconstructed  $t\bar{t}$  candidates in the  $t\bar{t}$  sample (1) and  $W+4$  jets background samples (2) and (3) described above. Fig. 1 shows the  $M_{t\bar{t}}$  distribution (upper) and  $M_{t\bar{t}}$  dependence of  $A_{FB}^{t\bar{t}}$  (lower). In the upper plot, the solid red, dashed blue and dotted green histograms show the differential cross sections in  $\text{fb}/\text{GeV}$  unit after event selection for the  $t\bar{t}$  signal (1),  $W+4j$  (3) and  $W+b\bar{b}+2j$  (2) background samples, respectively. Because of the large cross section of the  $W+4$  light-jets process that pass the first selection cuts of eqs.(4), 5.3pb with the fixed QCD coupling of  $\alpha_s = 0.171$ , the sample (3) gives the major background contribution of 1.4 pb even after the  $b$ -tagging requirement (7c).  $W+b\bar{b}+2j$  sample (2) gives 0.10 pb, while the leading-order  $t\bar{t}$  signal (1) gives 1.8 pb. All the distributions peak at  $M_{t\bar{t}} \sim 400$  GeV and decrease exponentially in high  $M_{t\bar{t}}$  region. The cross section of the  $W+4j$  background decreases more slowly than the other two samples. In the lower plot, the forward-backward asymmetry of the  $t\bar{t}$ ,  $W+4j$  and  $W+b\bar{b}+2j$  samples are shown separately as the circle-red, triangle-blue and rectangular-green points, respectively, with their error bars for the  $M_{t\bar{t}}$  bins of 350-450, 450-550, 550-650 and 650-950 GeV. As expected, the asymmetry of the  $t\bar{t}$  sample is consistent with zero in all bins since the sample is generated at tree level. The asymmetries of the  $W+4j$  and  $W+b\bar{b}+2j$  samples have finite values and increase monotonically with  $M_{t\bar{t}}$ ; the  $W+4j$  sample gives the largest asymmetry in all bins with values up to 0.15, while the  $W+b\bar{b}+2j$  sample gives the asymmetry of 0.02 to 0.04 as  $M_{t\bar{t}}$  grows from the 400 GeV bin to the 800 GeV bin.

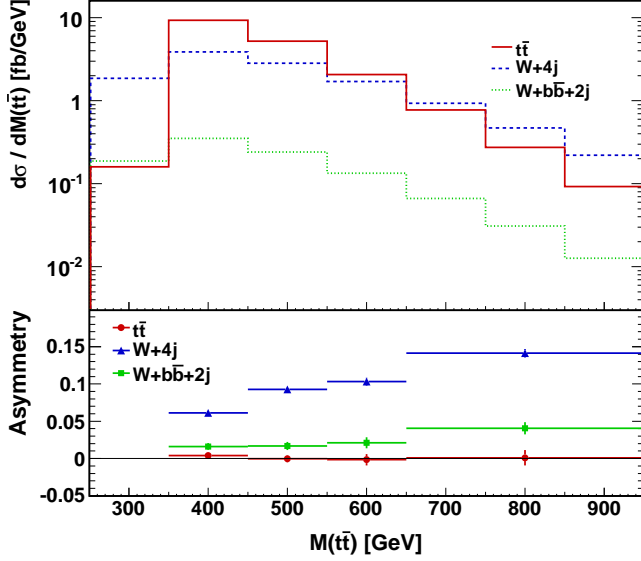


Figure 1: **Upper:**  $M_{t\bar{t}}$  distributions of the reconstructed  $t\bar{t}$  candidates in  $\text{fb}/\text{GeV}$  unit. The solid red, dashed blue and dotted green histograms show the differential cross sections after event selection in the  $t\bar{t}$ ,  $W+4j$  and  $W+b\bar{b}+2j$  samples, respectively. **Lower:** the  $M_{t\bar{t}}$  dependence of the top forward-backward asymmetries of the reconstructed  $t\bar{t}$  candidates. Asymmetries are evaluated in each bin; those of the last three bins are unified.

The positive asymmetry in the  $W+4$  jets events reflects the tendency of the  $W^+$  emission along the proton direction. We show in Fig. 2 the  $\Delta y$  distributions of the reconstructed  $t\bar{t}$  candidates in the  $t\bar{t}$  and  $W+4$  jets samples. Here and below, the “ $W+4$  jets” sample is the sum of the  $W+b\bar{b}+2j$  (2) and  $W+4j$  samples (3). The solid red histogram is for the  $t\bar{t}$  signal sample, which is symmetric about  $\Delta y = 0$  as expected for the tree-level QCD prediction. The dashed blue histogram gives the distribution of the total  $W+4$  jets background sample. Furthermore, the  $W+4$  jets sample is divided into three sub-samples, according to the jet component of the reconstructed leptonic-top candidates:  $l^+/\nu$ -gluon ( $l^+/\nu g$ ),  $l^+/\nu$ -quark ( $l^+/\nu q$ ) and  $l^+/\nu$ -antiquark ( $l^+/\nu \bar{q}$ ). The solid green, dash-dotted blue and dotted orange histograms show contributions of the  $l^+/\nu g$ ,  $l^+/\nu q$  and  $l^+/\nu \bar{q}$  sub-samples, respectively. Those histograms are normalized such that their integrals equal to the cross sections after event selection for the  $t\bar{t}$  candidates. In the upper plot for  $M_{t\bar{t}} > 450$  GeV, the  $W+4$  jets distribution clearly shows the positive asymmetry with two peaks around  $|\Delta y| \sim 1.5$  while the real  $t\bar{t}$  distribution has one peak around  $|\Delta y| \sim 0$ . The  $l^+/\nu q$  and  $l^+/\nu \bar{q}$  sub-sample distributions have their peak at  $\Delta y \sim 1.5$  and -1.5, respectively, while the  $l^+/\nu g$  sub-sample shows the two-peak distribution with the positive asymmetry. The positive asymmetry in the total  $W+4$  jets distribution as well as in the  $l^+/\nu q$  and  $l^+/\nu \bar{q}$  sub-samples are also recognizable in the lower plot for  $M_{t\bar{t}} < 450$  GeV.

The  $W^+$  emitted from a hard up quark in the proton often combines with the down quark in the  $u \rightarrow dW^+$

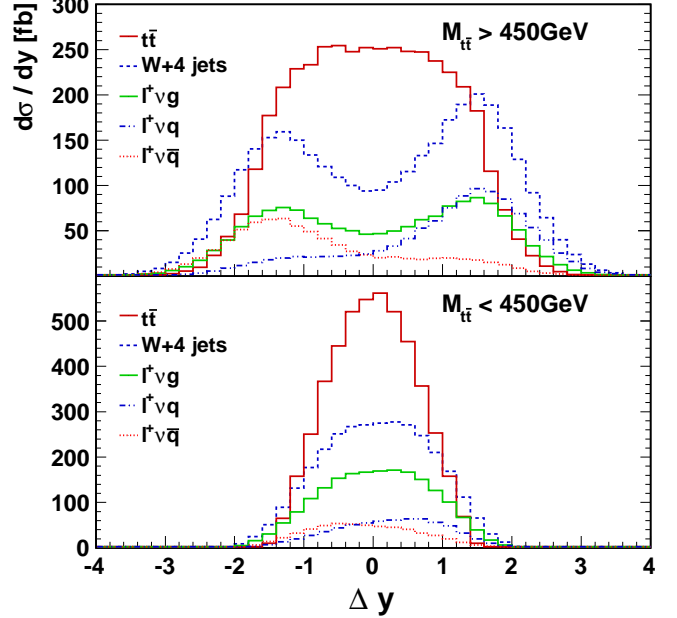


Figure 2:  $\Delta y$  distributions in  $\text{fb}$  unit. The  $W+4$  jets background is the sum of the  $W+b\bar{b}+2j$  (2) and  $W+4j$  (3) samples. The solid green, dash-dotted blue and dotted orange histograms show the contributions of sub-samples  $l^+/\nu g$ ,  $l^+/\nu q$  and  $l^+/\nu \bar{q}$  in the  $W+4$  jets sample, where the leptonic top quark is reconstructed from a  $l^+/\nu$ -gluon,  $l^+/\nu$ -quark and  $l^+/\nu$ -antiquark system, respectively. Histograms are normalized to the cross sections after event selection.

transition to form a fake “top” quark as a  $l^+/\nu$ -quark combination in Fig. 2, which tends to have the rapidity in the forward direction especially at high  $M_{t\bar{t}}$ . The forward-emitted  $W^+$  sometimes combines with a relatively ‘soft’ gluon to form a  $l^+/\nu g$  top candidate. The asymmetries of the  $W+4$  jets sample at high and low  $M_{t\bar{t}}$  in Fig. 2 are 11% and 6%, respectively, large enough to account for the observed asymmetry[1, 2] when combined with the QCD NLO prediction[3, 4, 5, 6] for the  $t\bar{t}$  signal events. However, such significant asymmetry in the  $W+4$  jets background events has not been reported by CDF[1] and D0[2] collaborations.

We note here that the  $\chi^2$  function of eq. (8) has been used to fix the combinatoric ambiguities only, and all the events that pass the selection cuts of eqs. (4) and (7) are used to obtain the above distributions. In real experiments, the reconstructed  $M_{l\nu}$ ,  $M_{jj}$ ,  $M_{bl\nu}$  and  $M_{bjj}$  which appear in eq. (8) distribute according to detector resolution and jet-finding algorithms, and can also depend on  $M_{t\bar{t}}$  since the average energy of the lepton and jets should be large for high  $M_{t\bar{t}}$ . We therefore examine the invariant mass distribution of the reconstructed top candidates in Fig. 3 with the same symbols as in Fig. 2. Even though none of the samples contains a real top quark, all the distributions have a peak around 150 – 200 GeV, at both  $M_{t\bar{t}} > 450$  GeV and  $M_{t\bar{t}} < 450$  GeV. Although in real experiments the parton-level invariant mass distributions in Fig. 3 should be smeared by hadronization and detector resolution as well as by the jet-finding process, the probability that the lower ( $< 150$  GeV) and higher ( $> 200$  GeV)

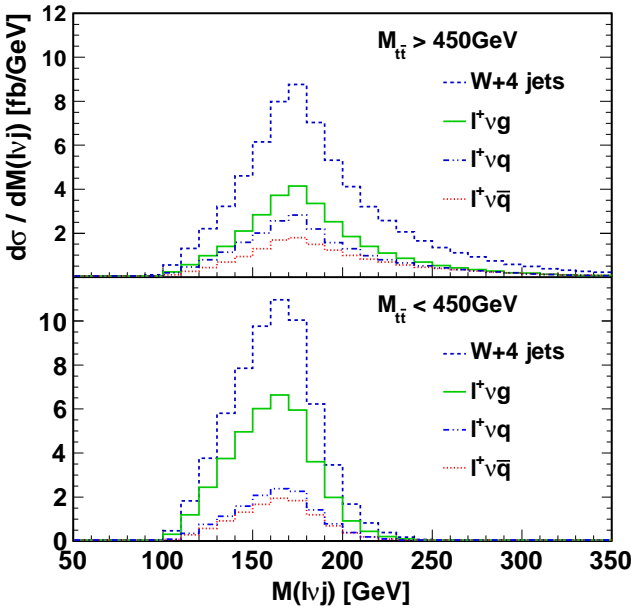


Figure 3: Invariant mass distributions of the reconstructed leptonic top in fb/GeV unit. The solid green, dash-dotted blue and dotted orange histograms show the contributions of sub-samples  $l^+\nu g$ ,  $l^+\nu q$  and  $l^+\nu \bar{q}$  in the  $W+4$  jets sample, where the leptonic top quark is reconstructed from a  $l^+\nu$ -gluon,  $l^+\nu$ -quark and  $l^+\nu$ -antiquark system, respectively. Histograms are normalized to the cross sections after event selection.

invariant mass events at the matrix-element level remain as the top quark candidates in experiments would be lower than that of those events in the 'top' mass region,  $150 \text{ GeV} < M_{l\nu j} < 200 \text{ GeV}$ . We therefore examine all the distributions after removing events where the reconstructed mass ( $M_{l\nu j}$ ) is below 150 GeV or above 200 GeV. None of the distributions shown in this report is affected significantly. For example, the forward-backward asymmetries for  $M_{t\bar{t}} > 450 \text{ GeV}$  and  $M_{t\bar{t}} < 450 \text{ GeV}$  after the  $M_{l\nu j}$  cut are 13 % and 5%, respectively, as compared to 11% and 6%, respectively, reported above from Fig. 2.

We further note that  $|V_{us}|^2 \sim 5\%$  of the forward  $l^+\nu q$  candidates have the  $s$ -quark, and  $|V_{ub}|^2 \sim 0.002\%$  the  $b$ -quark. Although these events may be statistically insignificant, jet flavor dependence of the  $b$ -(miss) tagging probability may be worth studying in the  $(l\nu j)$ -top-candidate events. All in all, we would like Tevatron experiments to look for the positive asymmetry in the  $W+4$  jets background events as a prediction of the SM at least in the matrix-element level. We believe that such serious studies of the background events will shed light on the  $t\bar{t}$  asymmetry issue.

In order to aid further discrimination of the  $W+4$  jets background events from the  $t\bar{t}$  signal, we examine two other kinematic distributions which are expected to differ significantly between the signal and the background. One is the transverse momentum distribution of the reconstructed top quark, as shown in Fig. 4 with the same symbols as in Fig. 2, i.e., solid red lines for the  $t\bar{t}$  signal and dashed blue lines for the  $W+4$  jets background. The dis-

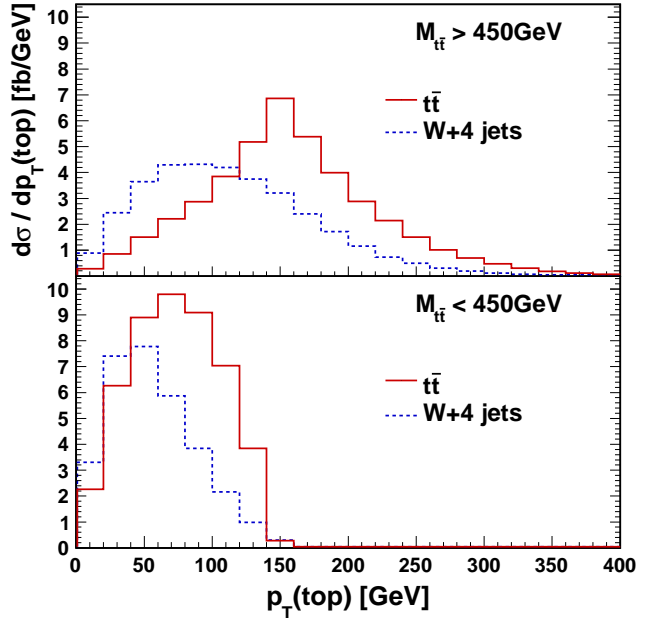


Figure 4: The transverse momentum distributions of the reconstructed top-quark candidates in fb/GeV unit. The solid red histograms show the distributions of the  $t\bar{t}$  signal events, and the dashed blue histograms give those of the  $W+4$  jets background events for  $M_{t\bar{t}} > 450 \text{ GeV}$  (upper) and  $< 450 \text{ GeV}$  (lower). Histograms are normalized to the cross sections after event selection.

tribution of the  $W+4$  jets events is softer than that of the  $t\bar{t}$  signal events; this is because the real top quark is produced via the s-channel  $q\bar{q}$  annihilation, whereas the top quark candidate in the  $W+4$  jets sample is formed with jets which are dominantly emitted via the t-channel gluon exchange. The difference between the  $t\bar{t}$  and  $W+4$  jets distribution is more evident at high  $M_{t\bar{t}}$  region since the mean top quark  $p_T$  from  $q\bar{q}$  annihilation grows linearly as  $M_{t\bar{t}}$ , while that from  $W+4$  jets background grows only logarithmically. The  $p_T$  of the reconstructed top quark may be a good discriminant between the signal and background especially at high  $M_{t\bar{t}}$ .

We also compare the transverse momentum distribution of the reconstructed  $t\bar{t}$  system,  $p_T(t\bar{t})$ . If  $W+4$  jets background is significant at high  $M_{t\bar{t}}$  region, the reconstructed  $t\bar{t}$  system should have significantly softer initial-state radiation than what is expected for the standard  $q\bar{q}$  annihilation processes for the  $t\bar{t}$  production. This is because the hard scale of the  $W+4$  jets process is set by the smallest  $p_T$  of the selected jets,  $\sim 20 \text{ GeV}$ , as compared to that of the  $t\bar{t}$  production process,  $\sim M_{t\bar{t}}/2$ . We try to simulate the difference using MadGraph[11] and Pythia[16]. For the  $t\bar{t}$  signals, we use the standard MLM matching scheme[17] with  $t\bar{t}+1$ -jet matrix elements for stable  $t$  and  $\bar{t}$  quarks. We allow Pythia to generate only initial-state radiation using the  $p_T$ -ordered shower[16]. The dashed, solid and dotted red histograms in Fig. 5 are obtained for the factorization scale of  $Q = M_{t\bar{t}}/n$  with  $n = 1, 2$  and  $4$ , respectively, when the parton shower is matched to the  $t\bar{t}+1$ -jet matrix elements at  $p_T(t\bar{t}) = M_{t\bar{t}}/6$ . For the  $W+4$  jets background, the dotted blue histogram is obtained with the scale of

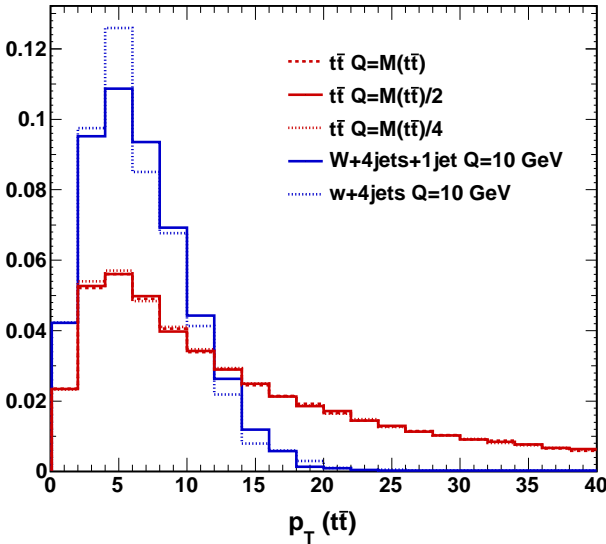


Figure 5: The transverse momentum distributions of the reconstructed  $t\bar{t}$  system in an arbitrary unit.  $Q$  is the factorization scale for the initial-state parton shower[16]. All histograms are normalized such that their integrals equal to one.

$Q = 10$  GeV, half of the jet selection  $p_T$  cut. The solid blue histogram is obtained where the initial-state shower is matched to the  $W+5$  jets matrix elements when the 5th-jet  $p_T$  is 10 GeV. Since we suppress final-state parton shower, our simulation is far from realistic; we believe, however, that the qualitative features of the difference in the initial-state-radiation effects between the  $t\bar{t}$  production and  $W+4$  jets events should be as large as indicated in Fig. 5, if one could separate final-state jets from initial-state ones. We therefore suggest that the softer-than-predicted  $p_T(t\bar{t})$  distribution reported by D0[2] can be a hint of the significant contamination of the  $W+4$  jets background in their  $t\bar{t}$  candidate events. Serious studies on the initial-state-radiation effects on the  $W+4$  jets backgrounds are hence desired in addition to the NLO contributions of the  $t\bar{t}+$  jet process as recently discussed in Ref.[18].

#### 4. Discussions and Conclusion

In this report we have studied properties of the  $W+4$  jets background for the  $t\bar{t}$  production events at the Tevatron by simulating the  $t\bar{t}$  event selection cuts to the background events at the matrix-element level. We find that those  $W+4$  jets background events which pass the selection cuts have the following peculiar properties:

- The rapidity difference ( $\Delta y = y_t - y_{\bar{t}}$ ) distribution is broader than that of the  $t\bar{t}$  events and has the large positive asymmetry at high  $M_{t\bar{t}}$ .
- The transverse momentum distribution of the top quark candidates is significantly softer than that of the real top quarks, especially at large reconstructed  $M_{t\bar{t}}$ .

- The transverse momentum distribution of the reconstructed  $t\bar{t}$  system is softer in  $W+4$  jets sample than that in the real  $t\bar{t}$  sample.

We suggest that the discrepancy in the  $p_T(t\bar{t})$  distribution found by D0 collaboration[2] may be explained by the significant contamination of the  $W+4$  jets backgrounds.

Since our analysis is based on the over-simplified identification of final-state partons as jets, the distributions presented in this report should not be regarded as realistic. Nevertheless, we would like to suggest experimentalists to re-examine their signal-to-background discriminants by using the matrix-element-level predictions for  $\Delta y$ ,  $p_T(\text{top})$  and  $p_T(t\bar{t})$  distributions as hints of possible background shapes, by noting that we do not yet have full control on the matched parton-shower predictions for multi-jet events at hadron colliders.

#### Acknowledgements

We wish to thank Yuji Takeuchi, Koji Sato and Suyong Choi for valuable discussions on the CDF and D0 analyses. Y.T. would like to thank the members of the CP3 at Universite catholique de Louvain for their warm hospitality, where a part of this work was done. He was also supported in part by Sokendai short-stay study abroad program. This work is supported in part by Grant-in-Aid for Scientific Research from the Japan Society for the Promotion of Science (No. 20340064).

#### References

- [1] T. Aaltonen, et al., Phys.Rev. D83 (2011) 112003.
- [2] V. M. Abazov, et al., Phys.Rev. D84 (2011) 112005.
- [3] J. H. Kuhn, G. Rodrigo, Phys.Rev. D59 (1999) 054017.
- [4] M. Bowen, S. Ellis, D. Rainwater, Phys.Rev. D73 (2006) 014008.
- [5] S. Dittmaier, P. Uwer, S. Weinzierl, Phys.Rev.Lett. 98 (2007) 262002.
- [6] L. G. Almeida, G. F. Sterman, W. Vogelsang, Phys.Rev. D78 (2008) 014008.
- [7] N. Kidonakis, Phys.Rev. D84 (2011) 011504.
- [8] W. Hollik, D. Pagani, Phys.Rev. D84 (2011) 093003.
- [9] T. Aaltonen, et al., Phys.Rev.Lett. 106 (2011) 171801.
- [10] V. Abazov, et al., Phys.Rev.Lett. 107 (2011) 011804.
- [11] J. Alwall, M. Herquet, F. Maltoni, O. Mattelaer, T. Stelzer, JHEP 1106 (2011) 128.
- [12] K. Hagiwara, J. Kanzaki, N. Okamura, D. Rainwater, T. Stelzer, Eur.Phys.J. C66 (2010) 477; K. Hagiwara, J. Kanzaki, N. Okamura, D. Rainwater, T. Stelzer, Eur.Phys.J. C70 (2010) 513.
- [13] K. Hagiwara, J. Kanzaki, Q. Li, N. Okamura, T. Stelzer, in preparation .
- [14] J. Kanzaki, Eur.Phys.J. C71 (2011) 1559.
- [15] The CDF collaboration, [http://www-cdf.fnal.gov/physics/new/top/confNotes/cdfnote\\_9724\\_public\\_v01-3.pdf](http://www-cdf.fnal.gov/physics/new/top/confNotes/cdfnote_9724_public_v01-3.pdf) (2009).
- [16] T. Sjostrand, S. Mrenna, P. Z. Skands, JHEP 0605 (2006) 026.
- [17] M. L. Mangano, M. Moretti, F. Piccinini, M. Treccani, JHEP 0701 (2007) 013.
- [18] K. Melnikov, A. Scharf, M. Schulze, Phys.Rev. D85 (2012) 054002.